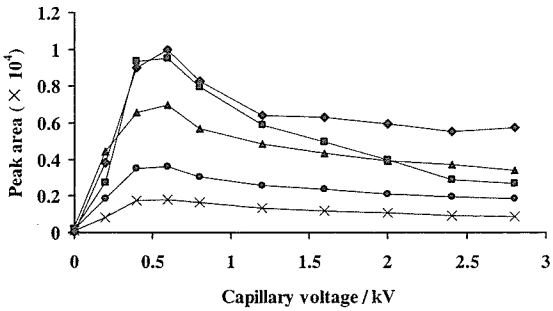

Fig. 5 Effect of capillary voltage on the peak area of PFCs

◆: PFOS; ■: PFOSA; ▲: PFOA; ●: PFNA; ×: PFDA

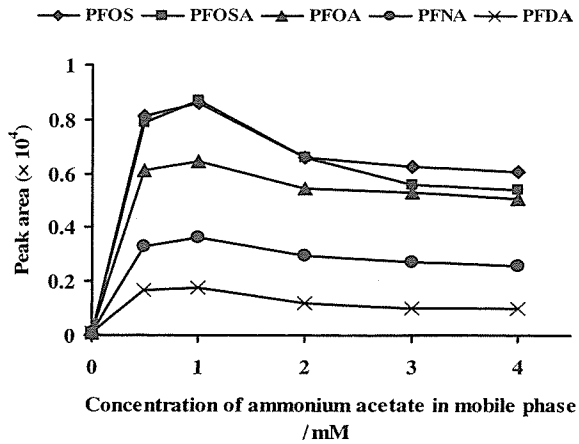

Fig. 6 Effect of concentration of ammonium acetate in mobile phase on the peak area of PFCs

◆: PFOS; ■: PFOSA; ▲: PFOA; ●: PFNA; ×: PFDA

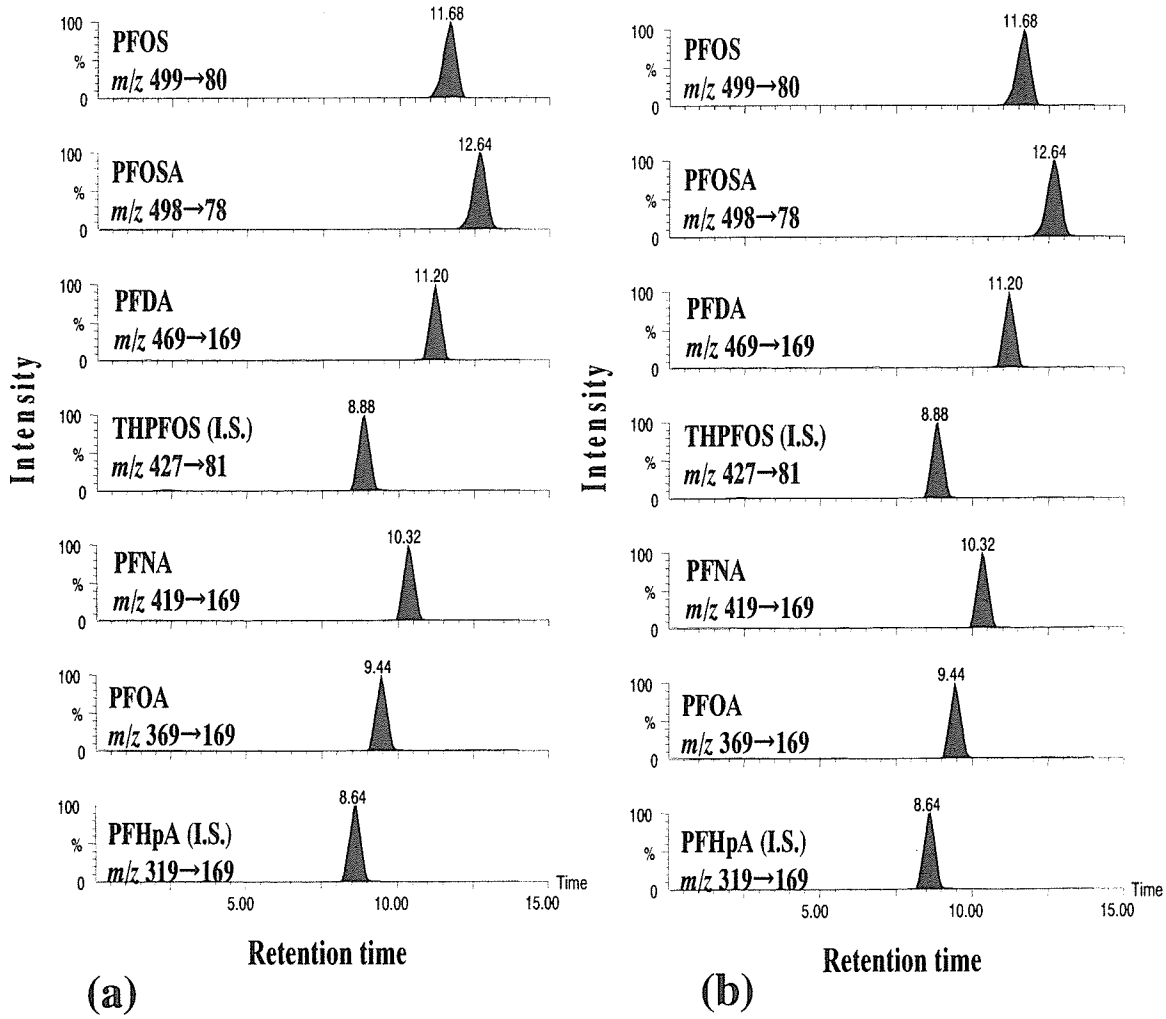

Fig. 7 MRM chromatograms of (a) a mixture of standards (PFOS, PFOSA, PFOA, PFNA, PFDA) and internal standards; (b) pooled human plasma with addition of 10 ng/ml PFCs

Table 2　Recovery levels of PFOS, PFOSA, PFOA, PFNA and PFDA in human plasma samples

Compound	Spiked amount/ ng ml^{-1}, human plasma sample	Average recovery, %	RSD, %
PFOS	5	99.3	3.0
	50	97.5	6.3
PFOSA	1	98.3	4.2
	10	105	4.2
PFOA	1	100	8.9
	10	97.3	4.8
PFNA	1	96.7	8.4
	10	94.7	3.1
PFDA	1	93.3	8.7
	10	103	4.7

$n = 6$

Table 3　Concentration of PFOS, PFOSA, PFOA, PFNA and PFDA in plasma samples from healthy volunteers

Volunteer	PFOS	PFOSA	PFOA	PFNA	PFDA
A (male)	5.6 ± 0.15	N.D.	1.7 ± 0.13	N.D.	N.D.
B (male)	17.7 ± 0.35	N.D.	2.8 ± 0.11	1.0 ± 0.05	N.D.
C (male)	21.3 ± 1.35	N.D.	4.6 ± 0.06	0.8 ± 0.05	N.D.
D (female)	2.1 ± 0.09	N.D.	0.7 ± 0.02	N.D.	N.D.
E (female)	10.4 ± 0.31	N.D.	2.4 ± 0.14	N.D.	N.D.
F (female)	15.1 ± 0.91	N.D.	1.9 ± 0.07	0.6 ± 0.02	N.D.

mean ± SD ng ml^{-1}, N.D.$<$ 0.5 ng ml^{-1}, $n = 3$

定が可能となった．先に報告したカラムスイッチング-HPLC/MS法[18)19)]と本法を比較すると，測定装置にMS/MSを用いることでバックグラウンドの影響を軽減することができ，回収率が93.3%以上と向上した．また，分析カラムに50 mmのODSカラムを用いたことで，測定時間を15分に短縮することができた．再現性に関しては，前報では，オンライン固相抽出の溶離液に水/メタノール混液を用いていたが，今回，50 mM酢酸・酢酸アンモニウム緩衝液（pH = 4.7)/メタノール混液を用いたことで，保持時間のRSD（%）値が1.1%以下と良好な結果が得られた．以上のことから，本法は前報[18)19)]に比べて迅速かつ高い分析精度でPFCsの測定が可能となった．更に本法をヒト血しょう試料に応用したところ，PFOS，PFOA及びPFNAを検出することができた．今後，本法が多くのヒト血液試料の分析に用いられることにより，大規模な疫学研究等が実施され，PFOS及びPFOS関連化合物のリスク評価に資するものと期待される．

文　献

1) J. P. Giesy, K. Kannan: *Environ. Sci. Technol.*, **35**, 1339 (2001).
2) K. Kannan, S. Corsolini, J. Falandysz, G. Oehme, S. Focardi, J. P. Giesy: *Environ. Sci. Technol.*, **36**, 3210 (2002).
3) K. Kannan, J. Newsted, R. S. Halbrook, J. P. Giesy: *Environ. Sci. Technol.*, **36**, 2556 (2002).
4) K. J. Hansen, H. O. Johnson, J. S. Eldridge, J. L. Butenhoff, L. A. Disk: *Environ. Sci. Technol.*, **36**, 1681 (2002).
5) S. Taniyasu, K. Kannan, Y. Horii, N. Hanari, N. Yamashita: *Environ. Sci. Technol.*, **37**, 2634 (2003).
6) J. R. Thibodeaux, R. G. Hanson, J. M. Rogers, B. E. Grey, B. D. Barbee, J. H. Richards, J. L. Butenhoff, L. A. Stevenson, C. Lau: *Toxicol. Sci.*, **74**, 369 (2003).
7) C. Lau, J. R. Thibodeaux, R. G. Hanson, J. M. Rogers, B. E. Grey, M. E. Stanton, J. L. Butenhoff, L. A. Stevenson: *Toxicol. Sci.*, **74**, 382 (2003).
8) T. Ikeda, K. Aiba, K. Fukuda, M. Tanaka: *J. Biochem.*, **98**, 475 (1985).
9) A. K. Sohlenius, K. Andersson, J. DePierre: *J. Biochem.*, **285**, 779 (1992).
10) Y. Kawashima, N. Uy-Yu, H. Kozuka: *J. Biochem.*, **261**, 595 (1989).
11) X. Han, T. A. Show, R. A. Kemper, G. W. Jepson: *Chem. Res. Toxicol.*, **16**, 775 (2003).
12) X. Han, P. M. Hinderliter, T. A. Show, G. W. Jepson: *Drug. Chem. Toxicol.*, **27**, 341 (2004).
13) S. Taniyasu, K. Kannan, Y. Horii, N. Hanari, N. Yamashita: *Environ. Sci. Technol.*, **37**, 2634 (2003).
14) G. W. Olsen, K. J. Hansen, L. A. Stevenson, J. M. Burris, J. H. Mandel: *Environ. Sci. Technol.*, **37**, 888 (2003).
15) K. Kannan, S. Corsolini, J. Falandysz, G. Fillmann, K. S. Kumar, B. G. Loganathan, M. A. Mohd, J. Olivero, J. H. Yang, K. M. Aldous: *Environ. Sci. Technol.*, **38**, 4489 (2004).
16) Z. Kuklenyik, J. A. Reich, J. S. Tully, A. M. Calafat: *Environ. Sci. Technol.*, **38**, 3698 (2004).

17) A. Karrman, B. B. Van, U. Jarnberg, L. Hardell, G. Lindstrom: *Anal. Chem.*, **77**, 864 (2005).
18) K. Inoue, F. Okada, R. Ito, M. Kawaguchi, N. Okanouchi, H. Nakazawa: *J. Chromatogr. B*, **810**, 49 (2004).
19) K. Inoue, F. Okada, R. Ito, S. Kato, S. Sasaki, S. Nakajima, A. Uno, Y. Saijo, F. Sata, Y. Yoshimura, R. Kishi, H. Nakazawa: *Environ. Health Perspect.*, **112**, 1204 (2004).

要　旨

近年，新たな環境汚染物質として注目されているパーフルオロオクタンスルホン酸（PFOS）及びPFOS関連化合物を対象としたヒト血しょう試料中の一斉分析法について検討した．本研究では，試料前処理法にカラムスイッチング方式を用いたオンライン固相抽出法を採用することで，除タンパクした血しょう試料中のパーフルオロ化合物（PFCs）を簡便な操作で測定することが可能となった．本法をヒト血しょう試料中PFCsの分析へ応用した結果，検出限界は，0.08～0.14 ng/ml（$S/N=3$）であり，ヒト血しょう試料中における定量限界は，すべての測定対象化合物において0.50 ng/mlとした．また，内標準物質にパーフルオロヘプタン酸（PFHpA）を用いることにより，回収率93.3% 以上｛相対標準偏差（RSD）≦8.9%｝と良好な回収率を得ることができた．このことから，本法は，ヒト血しょう試料中のPFCsの定量に応用できることが明らかとなった．

BUNSEKI KAGAKU Vol. 55, No. 12, pp. 955–961 (2006)

報　文

超臨界流体抽出-高速液体クロマトグラフィー/タンデム質量分析法によるハウスダスト中パーフルオロ化合物の定量

勝又　常信[1]，中田　彩子[1]，岩崎　雄介[1]，伊藤　里恵[1]，
斉藤　貢一[1]，中澤　裕之®[1]

パーフルオロ化合物（PFCs）は，テフロン加工や撥水剤などとして日常で広く使われているが，催奇形性や甲状腺ホルモン撹乱作用などが報告されており，ヒトへの暴露影響が懸念されている．本研究では，PFCsのヒトへの暴露源としてハウスダストに着目し，超臨界流体抽出法と高速液体クロマトグラフィー/タンデム質量分析法による，パーフルオロオクタンスルホン酸（PFOS）など4種類を測定対象とした高感度分析法の構築を検討した．本法によるハウスダスト中PFCsの検出限界は，0.58～0.72 ng/gであった．また添加回収試験の結果は，平均回収率97.9% 以上（相対標準偏差＜5.8%）と良好な結果が得られた．本法を一般家庭で得られたハウスダスト20検体の分析に適用したところ，PFOS，パーフルオロオクタン酸及びパーフルオロノナン酸がすべての検体から検出された．

1　緒　　言

パーフルオロオクタンスルホン酸（PFOS）やパーフルオロオクタン酸（PFOA）を代表とする，パーフルオロ化合物（PFCs）は直鎖状に並んだ炭素原子すべてにフッ素原子が結合しており，末端にスルホン酸基又はカルボン酸基を有する構造をしている（Fig. 1）．PFCsは「水を弾くと同時に油も弾く」という特殊な性質を持っており，PFOSは，界面活性剤，撥水剤及び消泡剤等として用いられている．このように，PFCsは我々の生活環境中に広く利用されてきたが，近年，環境汚染報告[1)~3)]や生物への影響[4)~6)]などが報告され，新たな環境汚染物質として注目されている．

PFOS及びPFOAは自然環境においてPFCs類縁物質の最終分解物であるとされ，非常に安定であることが報告されている[7)~9)]．PFCsのヒト血清中での半減期はPFOSが8.70年，PFOAが4.37年と長く[10)]，血しょうタンパク質と結合して血液中に蓄積しているという報告がされている[11)12)]．実験動物に対する影響としては，催奇形性，甲状腺ホルモンへの影響[4)5)]及び脂肪酸代謝障害の誘発[6)]があり，ヒト臍帯血を介しての胎児移行性が報告[13)]されている．そのため，ヒトへの影響が懸念されており，血液試料（血しょう，血清）[14)~16)]や肝臓[17)]といったヒト生体試料を用いた，PFCsのヒト暴露量評価が行われてきた．特にPFOSは報告されているほぼすべてのヒト血液から検出されており，PFOAも高頻度に検出されることが報告されている[14)~16)]．そのため，ヒト暴露源の解明が求められている．

現在，PFCsの環境汚染報告としては，汚泥[1)]，環境水[2)]，大気[3)]などがあるが，PFCsは非常に低濃度であり，暴露源として評価するのは困難である．そこで本研究では，日常生活環境に常に存在し，クロルピリホスやジクロルボスなどを含むハウスダスト[18)]に着目し，ハウスダスト中PFCsを測定することとした．ハウスダスト中のPFCsの測定と

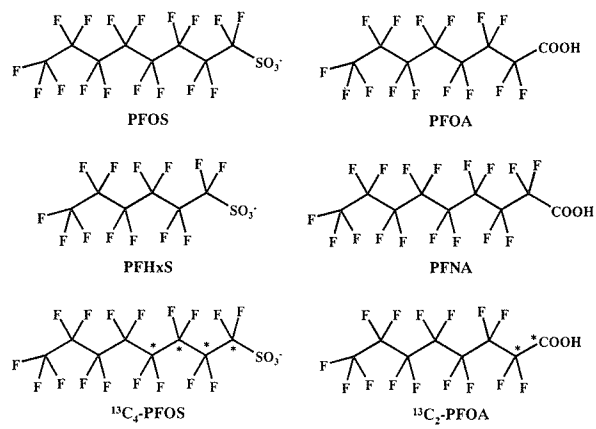

Fig. 1　Structures of analytes and the internal standard

PFOS: Perfluorooctanesulfonate; PFOA: Perfluorooctanoic acid; PFNA: Perfluorononanoic acid; PFHxS: Perfluorohexanesulfonate; $^{13}C_4$-PFOS: Perfluoro-[1, 2, 3, 4-$^{13}C_4$]octanesulfonic acid; $^{13}C_2$-PFOA: Perfluoro-[1, 2-$^{13}C_2$]octanoic acid (＊: stable carbon isotope, ^{13}C)

[1] 星薬科大学薬品分析化学教室：142-8501　東京都品川区荏原2-4-41

Table 1 Mass transitions monitored and MS/MS conditions

Compound	Precursor ion (m/z)	Product ion (m/z)	Cone voltage /(−V)	Collision energy /eV
PFOS	499	80	60	65
PFOA	413	369	14	11
PFNA	463	419	18	10
PFHxS	399	80	48	40
$^{13}C_4$-PFOS	503	80	60	65
$^{13}C_2$-PFOA	415	370	14	11

してMoriwakiらの報告[19]があり，これは，集塵(じん)バックに集めたダストからプラスチックや髪の毛などを除外したものを測定試料とし，メタノールにて超音波抽出を行っている．回収率はPFOSが89%，PFOAが73%となっており，検出値はPFOSが11～2500 ng/g，PFOAが70～3700 ng/gと報告している．本研究での抽出には食品中残留農薬の抽出に応用[20]されており，抽出溶媒に二酸化炭素を用いるため，労働衛生や測定環境に対し，非常に衛生的な超臨界流体抽出法を使用することとした．

環境及び生体試料中のPFCs測定には，高速液体クロマトグラフィー/質量分析法（LC/MS）[21)22)]及び高速液体クロマトグラフィー/タンデム質量分析法（LC/MS/MS）[1)～3)23)]が用いられている．ハウスダスト中には多くの化学物質が存在するため，測定法にLC/MS/MSを使用し，内標準物質に$^{13}C_4$-PFOS及び$^{13}C_2$-PFOAを用いることにより，高精度かつ高感度な分析法を構築する．

2 実　　験

2・1 試　薬

パーフルオロオクタンスルホン酸カリウム塩（$PFOS^-K^+$，>98%），パーフルオロオクタン酸（PFOA，>90%），パーフルオロノナン酸（PFNA，>98%）はFulka製，パーフルオロヘキサンスルホン酸ナトリウム塩（$PFHxS^-Na^+$，>98%）はWELLINGTON製を用いた．内標準物質として用いた$^{13}C_2$-PFOA（98.1%）はPerkin Elmer製，$^{13}C_4$-$PFOS^-Na^+$（>98%）はWELLINGTON製を用いた．超純水は日本ミリポア製Milli-Qの超純水装置で調製したものを用いた．アセトニトリル，メタノール，2-プロパノールは，和光純薬製HPLC用及び残留農薬試験用を使用した．ナイロンメンブランフィルター（0.2 μm，13 mm）は，日本ポール製を用いた．

2・2 標準溶液の調製

PFOS，PFOA，PFNAの標準液はそれぞれの標準品をアセトニトリルに溶解させ，1.0 mg/mlの溶液を調製した．PFHxSは0.05 mg/mlのメタノール溶液を用いた．標準溶液を水/メタノール＝50/50（v/v）で適宜希釈して，0.50～100 ng/mlの範囲で測定用試料を調製した．

2・3 装置及び分析条件

LC/MS/MSは，Waters製Quattro microシステムを用いた．注入量を20 μlとし，ガードカラムに関東化学製のMightysil RP-18 GPプレカラム（2.0×5 mm，5 μm）を用い，分析カラムにGLサイエンス製Inertsil ODS-3（2.1×50 mm，5 μm）を使用した．また，カラム恒温相は40℃に設定した．

超臨界流体抽出装置は，日本分光製SFC system SUPER 201型（送液ポンプ：SFE/C-201，カラム恒温相：CO-965，冷却器：CH-201，背圧制御装置：880-81）を用いた．また，カラム恒温相は40℃に設定した．

MS/MSのイオン化法は，エレクトロスプレーイオン化法（ESI）のネガティブイオンモードを採用し，検量線及び実試料の測定は，Multiple Reaction Monitoring（MRM）モードで行った．MS/MS条件としては，デソルベーション温度及びソース温度をそれぞれ350℃，100℃とし，コーンガス流量及びデソルベーションガス流量を50 l/hr，350 l/hrとした．また，キャピラリー電圧を−600 Vに設定した．コーン電圧及びコリジョンエネルギーをPFOS：−60 V，65 eV，PFOA：−14 V，11 eV，PFNA：−18 V，10 eV，PFHxS：−48 V，40 eV，$^{13}C_4$-PFOS：−60 V，65 eV，$^{13}C_2$-PFOA：−14 V，11 eVに設定した時，モニタリングイオンはそれぞれ，PFOS：m/z 499 → 80，PFOA：m/z 413 → 369，PFNA：m/z 463 → 419，PFHxS：m/z 399 → 80，$^{13}C_4$-PFOS：m/z 503 → 80，$^{13}C_2$-PFOA：m/z 415 → 370であった．測定条件の概要をTable 1に示す．

移動相は1 mM酢酸アンモニウムを添加した水/アセトニトリル（v/v）混液を用い，流量0.2 ml/minで送液し，測定時間0～9分にかけて，アセトニトリル含量を10～70%にグラジエント溶出して行った．

2・4 測定試料の調製法

ハウスダスト試料は，一般家庭の掃除機により，集塵バッグに集められたダストを用いた．得られたダストを1 mmふるいと75 μmふるいにて分け，粒子径75 μm～1.0 mmの領域を使用した．ハウスダストの定義として，生物学上ではダニの住む範囲と決められており，1 μm～1 mmの範囲となっている[24]．しかしながら，75 μm以下の

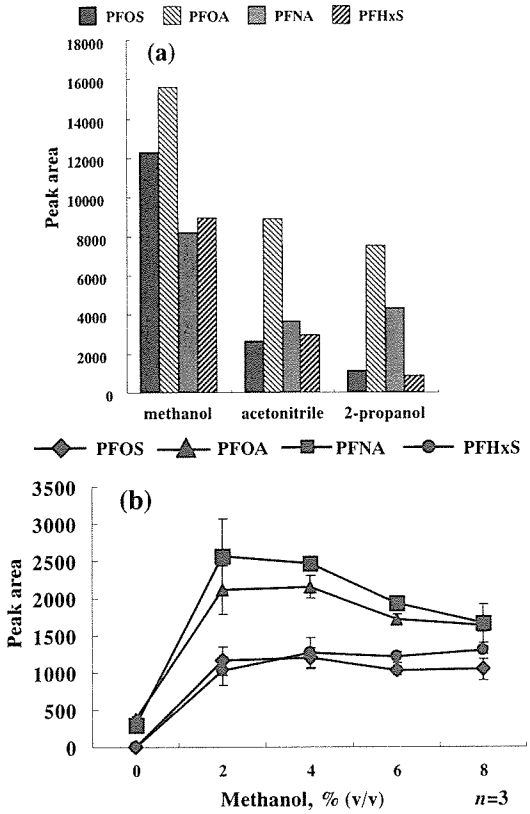

Fig. 2　Effect of (a) modifiers and (b) modifier concentration on extraction of PFCs for house dust

SFE conditions; (a) flow rate of CO_2: 4.80 ml/min, modifier: 0.20 ml/min (4 v/v%), pressure: 190 kg/cm^2, extraction time: 60 min; (b) flow rate of CO_2 and methanol: 5.0 ml/min, pressure: 190 kg/cm^2, extraction time: 60 min

ダストは大気中に浮遊している可能性があり，回収は困難であることと，屋外由来の塵が多く含まれることから 75 μm 以下のダストは対象外とした．また，1 mm 以上のダストにはプラスチック，ガラス，木くずや虫などが入っている可能性があり，0.5 g を採取した場合，粒子径のバラツキが考えられ，本研究では上限と下限を設けた．ハウスダスト試料を 0.5 g 採取し，超臨界流体抽出用セルに充填し，0.1 μg/ml に調製した内標準物質を 0.5 ml 添加した．抽出溶媒である二酸化炭素とモディファイヤーであるメタノールを 4 v/v% 添加し，合わせて流量 5.0 ml/min で 1 時間送液することで抽出した．抽出液を 55℃ の水浴上にて窒素気流下で蒸発乾固を行い，水/メタノール = 50/50 (v/v)，2.5 ml にて再溶解をした．ナイロンメンブランフィルター (0.2 μm) で沪過し，測定試料とした．

3　結果及び考察

3・1　超臨界流体抽出法の抽出条件の検討

3・1・1　モディファイヤーの影響　本研究では，抽出溶媒として超臨界二酸化炭素を用いた．メタノール，2-プロパノール，アセトニトリルから，適したモディファイヤーの検討を行った．それぞれ，4 v/v% 添加し，超臨界二酸化炭素と合わせて流量 5.0 ml/min で 1 時間送液し，PFCs の抽出率を比較した．結果より，モディファイヤーにメタノールを用いた場合が，抽出率が最大となった {Fig. 2 (a)}．他の溶媒に比べ，極性が高いメタノールを用いることにより，超臨界流体の溶解度が最適化されたと考えられる．次に，二酸化炭素に対するモディファイヤーの体積比の影響を検討した．メタノールを 0～8 v/v% 添加し，超臨界二酸化炭素と合わせて流量 5.0 ml/min になるように設定し，1 時間送液した．その結果，二酸化炭素とメタノールの体積比が 96 : 4 (v/v) のとき，最大の抽出が得られた {Fig. 2 (b)}．メタノールの体積比の増加に伴うピーク面積の減少は，溶解度の上昇により抽出溶媒に他の夾雑成分が溶解し，マトリックス効果が起きたと考えられる．

3・1・2　抽出圧力及び抽出時間の最適化　抽出圧力を 150～220 kg/cm^2 の間に設定し，抽出量を比較した．190 kg/cm^2 以上はほぼ平衡に達し，バラツキも少ないため，抽出圧力は 190 kg/cm^2 とした {Fig. 3 (a)}．得られた条件をもとに，抽出時間を検討した．60 分以上にて平衡に達しているため，最適抽出時間は 60 分とした {Fig. 3 (b)}．

3・2　MS/MS 測定条件の検討

PFCs 4 種類の標準品を用いて，MS/MS のイオン化について検討した．イオン化法に ESI を採用し，ネガティブイオンモードで測定したところ，PFOS においては $[M-K]^-$ イオンの m/z 499，PFHxS 及び $^{13}C_4$-PFOS に関しては $[M-Na]^-$ イオンである m/z 399 及び 504 の分子量関連イオンピークがそれぞれ確認され，PFOS，PFHxS 及び $^{13}C_4$-PFOS に関しては，m/z 499，399，504 をプレカーサーイオンとした．PFOA，PFNA 及び $^{13}C_2$-PFOA では，$[M-H]^-$ イオンである m/z 413，463，415 と $[M-COOH]^-$ イオンである m/z 369，419，370 が存在する．しかし，$^{13}C_2$-PFOA は 1 位の炭素が同位体原子に置換されているため，PFOA，PFNA 及び $^{13}C_2$-PFOA に関しては，$[M-H]^-$ イオンである m/z 413，463，415 に設定した．またプレカーサーイオンが開裂することで生じるプロダクトイオンは，それぞれ PFOS: m/z 499 → 80，PFOA: m/z 413 → 369，PFNA: m/z 463 → 419，PFHxS: m/z 399 → 80，$^{13}C_4$-PFOS: m/z 503 → 80，PFOA: m/z 415 → 370 とした．

酢酸アンモニウム添加量及びキャピラリー電圧の設定は，仲田らの報告[23]に基づき，酢酸アンモニウム添加量を 1 mM とし，キャピラリー電圧は −600 V に設定した．

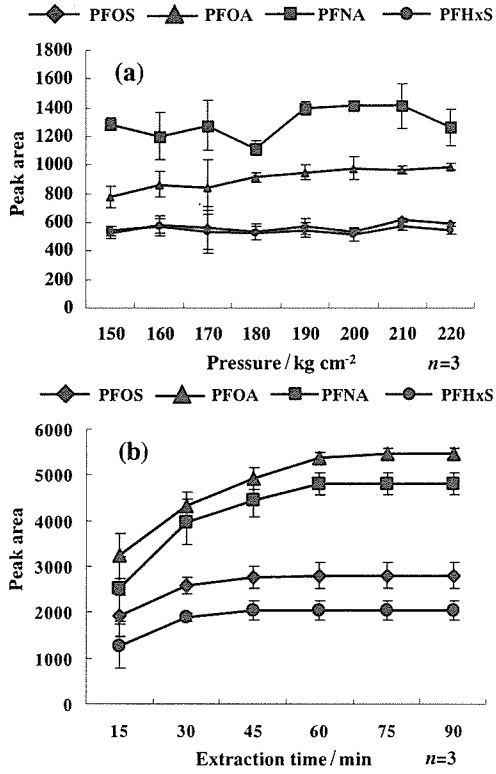

Fig. 3 Optimization of extraction (a) pressure and (b) time of PFCs for house dust

SFE conditions; (a) flow rate of CO_2: 4.80 ml/min, methanol: 0.20 ml/min (4 v/v%), extraction time: 60 min; (b) flow rate of CO_2: 4.80 ml/min, modifier: 0.20 ml/min (4 v/v%), pressure: 190 kg/cm^2

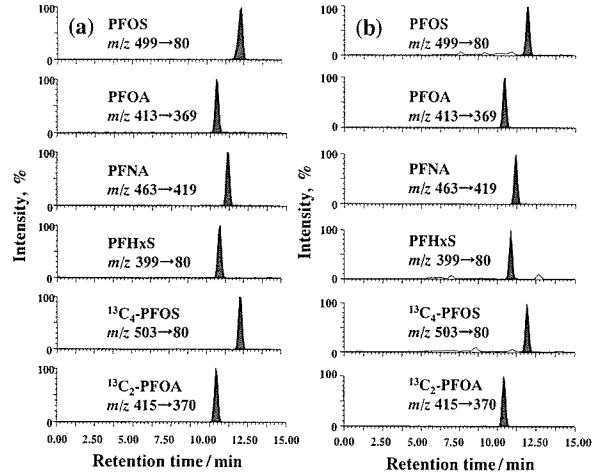

Fig. 4 MRM chromatograms of (a) a mixture of 5 ng/ml PFCs standards (PFOS, PFOA, PFNA, PFHxS) and internal standards; (b) house dust sample with addition of 50 ng/g PFCs

3・3 LC/MS/MS 測定条件の検討

PFCs4 種類の標準品を測定したところ，Fig. 4 (a) に示したクロマトグラムのようにすべての化合物が 15 分以内に良好に分離された．ハウスダスト試料をセルに詰め，50 ng/ml の標準溶液とサロゲート物質を加え，抽出を行った．クロマトグラムにおいても，他の夾雑物質の影響を受けることなく良好に相互分離することが可能であった {Fig. 4 (b)}．また，ハウスダスト試料における検出限界を繰り返し測定 ($n = 8$) にて求めたところ，PFOS: 0.58 ng/g，PFOA: 0.72 ng/g，PFNA: 0.65 ng/g，PFHxS: 0.63 ng/g となり，定量範囲は，2.5～500 ng/g であった．

3・4 添加回収試験

添加回収試験は，各測定対象化合物を異なる濃度レベルで添加したハウスダスト試料 0.5 g に 100 ng/ml の内標準物質溶液を 0.5 ml 加え，超臨界抽出を行った．得られた抽出液を窒素気流下で蒸発乾固させ，水/メタノール = 50/50 (v/v)，2.5 ml で再溶解した．再溶解液 1 ml をナイロンメンブランフィルター (0.2 μm) に通し，測定に供した．絶対検量線法にて回収率を求めたところ，56.1～79.6% {相対標準偏差 (RSD) ≦ 15.8%} という結果になった．これは，試料として用いたハウスダストは様々な化学物質が入っているため，絶対検量線法にて定量した場合，マトリックス効果により，回収率や再現性の低下などを引き起こしたと考えられる．そのため，本研究においては内標準法による定量を行った．PFOS 及び PFHxS のサロゲート物質として $^{13}C_4$-PFOS を用い，PFOA 及び PFNA の補正には $^{13}C_2$-PFOA を使用した．サロゲート物質で補正した回収率を算出した結果，平均回収率 97.9% 以上 (RSD ≦ 5.8%) となった (Table 2)．

また，Moriwaki らの報告に従い，ハウスダスト 0.5 g を 50 ml のポリプロピレンチューブに詰め，メタノール 10 ml とサロゲート 0.5 ml を添加し，1 時間超音波にて抽出を行った．本研究と同じ測定条件下で添加回収を行った結果，平均回収率 91.5～116.7% (RSD ≦ 8.3%，$n = 3$) となった．著者らの研究においても同等の回収率が得られているため，本分析法の有用性及び正確性が確認できた．

3・5 実試料の測定

本法を一般家庭から得られたハウスダスト試料，20 検体に適用し，ハウスダスト中の PFCs を測定した (Table 3)．すべての検体から PFOS，PFOA 及び PFNA が検出され，検出範囲は PFOS: 7.0～41 ng/g，PFOA: 18～89 ng/ml 及び PFNA: 5.5～69 ng/g であった．また，PFHxS に関しても 8 検体から 2.5～5.5 ng/ml の範囲で検出された．PFCs 間の相関は確認できなかったが，ほとんどのハウスダスト試料において，PFOA 濃度が PFOS 濃度より高いことが明らかとなった．一方，ヒト生体試料中では PFOS 濃度が PFOA 濃度よりも一般に高いと報告され

Table 2　Recovery levels of PFOS, PFOA, PFNA and PFHxS in house dust

Analyte	Spiked amount /ng g^{-1}	Concentration /ng g^{-1}	Average recovery ,%	RSD ,%
PFOS	50	64 ± 2.7	101.7	5.4
	250	278 ± 7.1	106.0	2.7
	0	13 ± 0.8		
PFOA	50	78 ± 2.2	102.1	4.4
	250	280 ± 8.3	101.5	3.3
	0	27 ± 0.9		
PFNA	50	55 ± 0.5	99.9	1.1
	250	257 ± 2.2	100.8	1.1
	0	5.5 ± 0.3		
PFHxS	50	53 ± 1.1	99.4	2.2
	250	248 ± 14.2	97.9	5.8
	0	3.0 ± 0.2		

n = 6

Table 3　Concentration of PFOS, PFOA, PFNA and PFHxS in house dust

Sample number	PFOS	PFOA	PFNA	PFHxS
1	41	89	35	ND
2	38	46	18	ND
3	37	20	6.0	ND
4	32	40	69	ND
5	29	64	11	3.0
6	28	51	43	ND
7	28	45	69	5.5
8	22	28	28	ND
9	21	53	9.0	2.5
10	20	40	13	ND
11	18	29	49	3.0
12	17	33	11	ND
13	17	33	8.0	ND
14	17	23	9.5	ND
15	14	26	14	ND
16	13	56	63	ND
17	13	34	8.0	ND
18	13	29	21	3.5
19	13	27	5.5	3.0
20	7.0	18	6.5	4.5

(ng/g, ND < 2.5 ng/g)

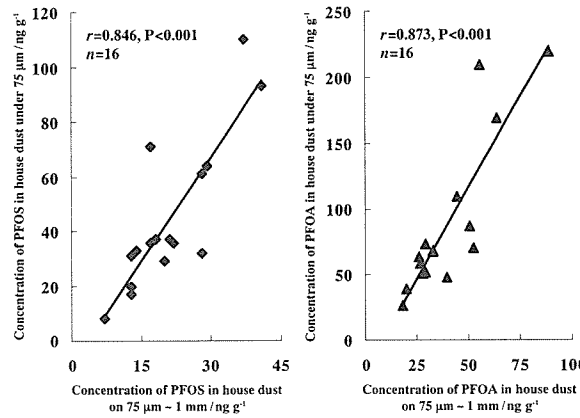

Fig. 5　Comparison of the PFCs concentration between particles

ている．これは，PFOS の方が体内半減期が長い[10]ことや，最終分解物が PFOA となる PFCs が多い[9]ことが考えられる．また，Moriwaki らの報告と比較すると，PFOS，PFOA に関して，本分析法はハウスダスト中濃度が低いが，これは，Moriwaki らの研究では髪の毛や，プラスチックなどを取り除いたものを測定試料としており，粒子径の小さなハウスダストも同時に分析していると考えられる．そのため，ハウスダストのサンプリング時に得られた粒子径 75 μm 以下のハウスダストにおいても本分析法を適用し，定量を行った．PFOS 及び PFOA の濃度について比較した結果（Fig. 5），粒子径の大きいものと小さいもので高い相関が得られ，粒子径 75 μm 以下のハウスダストは，高濃度に PFCs を含んでいることが確認された．これは，粒子径が縮小することにより，表面積は増大し，付着している化学物質の量が増大したと考えられる．そのため，Moriwaki らの報告と比較すると，ハウスダストに含まれる PFCs 濃度に差が生じたと考察できる．

4　結　　言

本分析法では，前処理に超臨界流体抽出法を行い，測定機器に LC/MS/MS を用いることによりハウスダスト中 PFCs の定量が可能となった．本研究で得られた結果より，本分析法はハウスダスト中 PFCs 濃度の定量法として有用であることが示唆された．また，本分析法によるハウスダスト中 PFCs の濃度は，環境水[2]，大気[3]といった環境試料と比較すると非常に高濃度であることが確認された．このことより，ハウスダストは PFCs のヒト暴露源として考えられる．今後，本分析法を用いて，ハウスダストからの暴露量評価が望まれる．

文　献

1) H. F. Schroder: *J. Chromatogr. A*, **1020**, 131 (2003).
2) K. J. Hansen, H. O. Johnson, J. S. Eldridge, J. L. Butenhoff, L. A. Dick: *Environ. Sci. Technol.*, **36**, 1681 (2002).
3) K. Sasaki, K. Harada, N. Saito, T. Tsutsui, S. Nakanishi, H. Tsuzuki, A. Koizumi: *Bull. Environ. Contam. Toxicol.*, **71**, 408 (2002).
4) J. R. Thibodeaux, R. G. Hanson, J. M. Rogers, B. E. Grey, B. D. Barbee, J. H. Richards, J. L. Butenhoff, L. A. Stevenson, C. Lau: *Toxicol. Sci.*, **74**, 369 (2003).
5) C. Lau, J. R. Thibodeaux, R. G. Hanson, J. M. Rogers, B. E. Grey, M. E. Stanton, J. L. Butenhoff, L. A. Stevenson: *Toxicol. Sci.*, **74**, 382 (2003).
6) J. W. Davis (II), J. P. Vanden Heuvel, R. E. Peterson: *Lipids*, **26**, 857 (1991).
7) J. P. Giesy, K. Kannan: *Environ. Sci. Technol.*, **35**, 1339 (2001).
8) K. Kannan, S. Corsolini, J. Falandysz, G. Oehme, S. Focardi, J. P. Giesy: *Environ. Sci. Technol.*, **36**, 3210 (2002).
9) C. C. Lange: "*The Aerobic Biodegradation of N-EtFOSSE Alcohol by the Microbial Actuvity Present in Municipal Waster Treatment Sludge*", Biodegadation Study Report, (2001), (Study Sponsor: 3M Company, US).
10) J. M. Burris, J. K. Lundberg, G. Olsen, C. Simpson, J. Mandel: "*Determination of serum half-five of several fluorochemicals, Interrim Report #2.*", (2002), (Study Sponsor: 3M Company, US).
11) X. Han, P. M. Hinderliter, T. A. Show, G. W. Jepson: *Drug. Chem. Toxicol.*, **27**, 341 (2004).
12) X. Han, T. A. Show, R. A. Kemper, G. W. Jepson: *Chem. Res. Toxicol.*, **16**, 775 (2003).
13) K. Inoue, F. Okada, R. Ito, S. Kato, S. Sasaki, S. Nakajima, A. Uno, Y. Saijo, F. Sata, Y. Yoshimura, R. Kishi, H. Nakazawa: *Environ. Health Perspect.*, **112**, 1204 (2004).
14) G. W. Olsen, J. M. Burris, J. H. Mandel, L. R. Zobel: *J. Occup. Environ. Med.*, **41**, 799 (1999).
15) K. J. Hansen, L. A. Clemen, M. E. Ellefson, H. O. Johnson: *Environ. Sci. Technol.*, **35**, 766 (2001).
16) G. W. Olsen, T. R. Church, J. P. Miller, J. M. Burris, K. J. Hansen, J. K. Lundberg, J. B. Armitage, R. M. Herron, Z. Medhdizadehkashi, J. B. Nobiletti, E. M. O'Neill, J. H. Mandel, L. R. Zobel: *Environ. Health Perspect.*, **111**, 1892 (2003).
17) H. F. Schroder: *J. Chromatogr. A*, **1020**, 131 (2003).
18) K. Roinestad, J. Louis, J. Rozen: *J. AOAC int.*, **76**, 1121 (1993).
19) H. Moriwaki, Y. Takata, R. Arakawa: *J. Environ. Monit.*, **5**, 753 (2003).
20) A. Aguilera, M. Rodriguez, M. Brotons, M. Boulaid, A. Valverde: *J. Agric. Food Chem.*, **53**, 9374 (2005).
21) C. Tseng, L. Liu, C. Chen, W. Ding: *J. Chromatogr. A*, **1**, 119 (2005).
22) A. Karrman, B. B. Van, U. Jarnberg, L. Hardell, G. Lindstrom: *Anal. Chem.*, **77**, 864 (2005).
23) 仲田尚夫，中田彩子，岡田文雄，伊藤里恵，井之上浩一，斉藤貢一，中澤裕之：分析化学 (*Bunseki Kagaku*), **54**, 877 (2005).
24) 森谷清樹訳: "ハウス・ダストの生物学　虫，ダニ，カビの生態・居住環境の衛生のために", (1990), (西村書店); Johanna E. M. H. van Bronswijk: "*House Dust Biology for allergists, acarologists, and mycologists*", (1981), (NIB Publishers, Zeist, The Ntherlands).

Determination of Perfluorochemicals in House-Dust by LC/MS/MS after Supercritical Fluid Extraction

Tsunenobu KATSUMATA[1], Ayako NAKATA[1], Yusuke IWASAKI[1], Rie ITO[1], Koichi SAITO[1] and Hiroyuki NAKAZAWA[1]

[1] Department of Analytical Chemistry, Hoshi University, 2-4-41, Ebara, Shinagawa-ku, Tokyo 142-8501

(Received 21 July 2006, Accepted 18 October 2006)

The purpose of this study is to find the exposure sources of perfluorochemicals (PFCs). We have developed a method for measuring 4 PFCs (perfluorooctanesulfonate; PFOS, perfluorooctanoic acid; PFOA, perfluorononanoic acid; PFNA and perfluorohexanesulfonate; PFHxS) in house dust using supercritical fluid extraction (SFE) and based on high-performance liquid chromatography/tandem mass spectrometry. The mean extracted recovery assessed at two different concentrations (50 and 250 ng/g in house dust) was more than 97.9%. The assay was linear over the range 2.5～500 ng/g. The method detection limits were assessed as being 0.58 ng/g to 0.72 ng/g. We determined the concentrations of PFCs in 20 house-dust samples for investigating of the exposure source. The compounds were detected in all dust samples and the ranges were 7.0～41 ng/g for PFOS, 18～89 ng/g for PFOA and 5.5～69 ng/g for PFNA. PFHxS was determined in 8 samples (2.5～5.5 ng/g). Based on our experiments, house-dust might be one of the human exposure sources for PFCs. The developed method can be applied to the determination of PFCs in house dust samples for monitoring human exposure sources.

Keywords : perfluorooctanesulfonate; perfluorooctanoic acid; perfluorochemicals; MS/MS; house dust; supercritical fluid extraction; exposure souses.

STEM CELLS

STEM CELL GENETICS AND GENOMICS

Dimethyl Sulfoxide Has an Impact on Epigenetic Profile in Mouse Embryoid Body

MISA IWATANI, KOHTA IKEGAMI, YULIYA KREMENSKA, NAKA HATTORI, SATOSHI TANAKA, SHINTARO YAGI, KUNIO SHIOTA

Laboratory of Cellular Biochemistry, Department of Animal Resource Sciences/Veterinary Medical Sciences, The University of Tokyo, Tokyo, Japan

Key Words. Dimethyl sulfoxide • DNA methylation • Epigenetics • Differentiation • DNA methyltransferase

ABSTRACT

Dimethyl sulfoxide (DMSO), an amphipathic molecule, is widely used not only as a solvent for water-insoluble substances but also as a cryopreservant for various types of cells. Exposure to DMSO sometimes causes unexpected changes in cell fates. Because mammalian development and cellular differentiation are controlled epigenetically by DNA methylation and histone modifications, DMSO likely affects the epigenetic system. The effects of DMSO on transcription of three major DNA methyltransferases (Dnmts) and five well-studied histone modification enzymes were examined in mouse embryonic stem cells and embryoid bodies (EBs) by reverse transcription-polymerase chain reaction. Addition of DMSO (0.02%–1.0%) to EBs in culture induced an increase in Dnmt3a mRNA levels with increasing dosage. Increased expression of two subtypes of Dnmt3a in protein levels was confirmed by Western blotting. Southern blot analysis revealed that DMSO caused hypermethylation of two kinds of repetitive sequences in EBs. Furthermore, restriction landmark genomic scanning, by which DNA methylation status can be analyzed on thousands of loci in genic regions, revealed that DMSO affected DNA methylation status at multiple loci, inducing hypomethylation as well as hypermethylation depending on the genomic loci. In conclusion, DMSO has an impact on the epigenetic profile: upregulation of Dnmt3a expression and alteration of genome-wide DNA methylation profiles with phenotypic changes in EBs. STEM CELLS *2006;24:2549–2556*

INTRODUCTION

Dimethyl sulfoxide (DMSO), an amphipathic molecule, is one of the most commonly used chemicals in the biological and medical sciences as a solvent for water-insoluble substances and a cryopreservant for various cell lines. It has multiple effects on cellular functions (e.g., metabolism and enzymatic activity) and on cell growth by affecting cell cycle and apoptosis [1]. It also changes cell fates by inducing differentiation of various types of cells [1–4] and promoting blastocyst formation in animal cloning [5].

Mammalian development and cellular differentiation are controlled by DNA methylation; the developmentally essential genes *Oct-4* and *Sry* are controlled to be expressed during a limited period of development by DNA methylation [6, 7]. Methylation is the sole modification of the vertebrate genome and occurs mainly at the 5-position of cytosines in cytosine-guanine (CpG) dinucleotides [8]. The modification is involved in epigenetic regulation of gene function, which is "mitotically and/or meiotically heritable, and can not be explained by changes in DNA sequences" [9]. Epigenetic systems regulate various genetic functions, including chromosomal stability, repression of transposable elements, and gene silencing [10–12] of developmentally regulated genes and genes expressed in a tissue-specific manner [13, 14]. Tissue-dependent and differentially methylated regions (T-DMRs) have been found in CpG-rich, unique sequences, including tissue-specific genes. The changes in genome-wide DNA methylation status of such T-DMRs provide every cell or tissue a unique DNA methylation profile consisting of methylated and unmethylated T-DMRs [15–17].

In the establishment and maintenance of the proper DNA methylation patterns in the mammalian genome, DNA methyltransferases (Dnmts) play critical roles. To date, five Dnmts, Dnmt1, 2, 3a, 3b, and 3L, have been identified. Because in vitro enzymatic activity is lacking in Dnmt2 and 3L [18, 19], only Dnmt1, Dnmt3a, and Dnmt3b have been intensively studied [20,

Correspondence: Kunio Shiota, D.V.M, Ph.D., Laboratory of Cellular Biochemistry, Department of Animal Resource Sciences/Veterinary Medical Sciences, The University of Tokyo, 1-1-1 Yayoi, Bunkyo-ku, Tokyo, 113-8657, Japan. Telephone: +81-3-5841-5472; Fax: +81-3-5841-8189; e-mail: ashiota@mail.ecc.u-tokyo.ac.jp Received August 31, 2005; accepted for publication July 1, 2006; first published online in STEM CELLS *EXPRESS* July 13, 2006. 1066-5099/2006/$20.00/0 doi: 10.1634/stemcells.2005-0427

21]. DNA methylation is associated with histone modifications in epigenetically regulated regions [20, 22–24]. Histone modifications were mediated by the following enzymes: G9a, Suv39h1, and Suv39h2 are histone H3 lysine nine (H3-K9) methyltransferases [12]; mDot1 is an H3-K79 methyltransferase [25]; and Sir2α is a class III histone deacetylase [26]. These enzymes and Dnmts coordinate the epigenetic systems.

Mutations in genes of epigenetic factors have been implicated as the causes of various diseases. Mutations in DNMT3b are associated with ICF syndrome (immunodeficiency, centromere instability, and facial abnormalities) [27], and those in MeCP2 are associated with Rett syndrome [28]. Epigenetic abnormalities have been reported in cloned animals [29–31] and cancerous cells [32] and are also caused by chemicals that are called "epimutagens" [33].

Based on these observations, we hypothesized that the effects on cell fate by DMSO should be interpreted by its effects on the epigenetic systems. We examined this hypothesis by using mouse embryonic stem cells (ESCs) and embryoid bodies (EBs). Differentiation of ESCs into EBs has been used as a model of normal and abnormal mammalian development [34]. It is also a suitable model for monitoring epigenetic modifications because, during differentiation from ESCs, EBs establish a specific DNA methylation profile associated with both hypermethylation and hypomethylation at multiple loci [16]. In this study, mRNA levels of epigenetic regulators, including Dnmts and histone modification enzymes, were analyzed. We also investigated a genome-wide DNA methylation profile in EBs to examine the effects of quantitative changes in an enzyme's expression.

Materials and Methods

Culture of ESCs, EBs, and DMSO Treatment

The ESC lines (MS12) derived from C57BL/6 strain mice [35] were cultured on embryonic fibroblast feeder cells with ESC medium: Dulbecco's modified Eagle's medium (DMEM; Invitrogen, Carlsbad, CA, http://www.invitrogen.com) supplemented with 15% fetal bovine serum and 1,000 U/ml of leukemia inhibitory factor (LIF; ESGRO, Chemicon International, Temecula, CA, http://www.chemicon.com). At passage 18, ESCs were treated with or without 0.1% (vol/vol) DMSO (Wako Pure Chemicals, Osaka, Japan, http://www.wako-chem.co.jp/english) for 4 days and harvested. EBs were induced by culturing ESCs at passage 16 without a feeder layer and LIF in bacteriological Petri dishes and simultaneously treated with or without DMSO. They were cultured under DMSO treatment for 4 days in EB medium:DMEM (Invitrogen) supplemented with 10% fetal bovine serum and then collected for nucleic acids and protein extractions.

RNA Extraction and Reverse Transcription-Polymerase Chain Reaction

Total RNA was purified from cultured ESCs and EBs using TRIzol reagent (Invitrogen) according to the manufacturer's instructions. For reverse transcription-polymerase chain reaction (RT-PCR), first-strand cDNA was synthesized from 1.0 μg of total RNA using a Superscript first-strand synthesis system with random hexamer primers (Invitrogen). RT-PCR was performed with rTaq polymerase (TOYOBO, Tokyo, http://www.toyobo.co.jp/e) except in the case of Dnmt3a, which was amplified with Immolase (BIOLINE, London, http://www.bioline.com). Sets of primer sequences for RT-PCR were as follows: Dnmt1: 5′-CAGGAGTGTGTGAGGGAG-3′ and 5′-GGTGTCACTGTCCGACTTGC-3′, Dnmt3a: 5′-ACCCATGCCAAGACTCACCTTC-3′ and 5′-TCCACCTTCTGAGACTCTCCAG-3′, Dnmt3b: 5′-TCAGACACGAAGGATGCTCC-3′ and 5′-ACAGGGTACTCCTGCACATG-3′, G9a: 5′-TTTGGCCATGAGGCTGTT-3′ and 5′-CCAGATGCATGTCATCACTCA-3′, Suv39h1: 5′-GGAGAAAGATGGCGGAAA-3′ and 5′-GACAAGAAAGCTTGGCTAGT-3′, Suv39h2: 5′-TCTTTGGCGACGAGTGTG-3′ and 5′-AGAATCTGGCCATCCTTTCC-3′, Sir2α: 5′-CTGACGACTTCGACGACGAC-3′ and 5′-TGCTGAACAAAAGTATATGGACCTATC-3′, mDot1: 5′-AACTATGTCCTGATCGACTACG-3′ and 5′-TCCTCTGTCATCTTGATCTCATC-3′, and β-actin: 5′-TTCTACAATGAGCTGCGTGTGG-3′ and 5′-ATGGCTGGGGTGTTGAAGGT-3′. The thermocycling program used with rTaq polymerase was an initial cycle of 95°C for 1 minute, followed by 30 cycles of 94°C for 30 seconds, and 30 seconds at the following annealing temperatures: 58°C for β-actin, 60°C for Suv39h1, 62°C for Dnmt1 and mDot1, and 65°C for Dnmt3b, G9a, Suv39h2, and Sir2α and then 72°C for 1 minute. RT-PCR for Dnmt3a using Immolase was performed with an initial cycle of 95°C for 10 minutes, followed by 30 cycles of 94°C for 30 seconds, 65°C for 30 seconds, and 72°C for 1 minute. A digitized image of ethidium bromide-stained gel was analyzed by densitometry with NIH Image 1.61 software (National Institutes of Health, Bethesda, MD, http://www.nih.gov).

Real-Time Quantitative RT-PCR

Expression of Dnmt3a was monitored by SYBR Green I in SYBR Green PCR Master Mix (Applied Biosystems, Foster City, CA, http://www.appliedbiosystems.com) on a ABI PRISM 7500 or 7900 HT sequence detection system (Applied Biosystems) according to the manufacturer's protocol. Nine nanomolar each of forward and reverse primers described above for Dnmt3a or β-actin and 1 μl and 0.5 μl of cDNAs were used for Dnmt3a and β-actin, respectively, in 20 μl. A standard curve was established by a dilution series of cDNA to estimate mRNA levels. Correlation values (r^2) of the standard curve were 0.98 and 0.99 for Dnm3a and β-actin, respectively. The slope of the standard curve was determined to calculate PCR efficiency using the equation: PCR efficiency = $10^{-1/\text{slope}} - 1$. The values for Dnmt3a and β-actin were 1.04 and 1.00, respectively. Quantitative expression level was calculated using the following equation: the value = $1/(1 + \text{PCR efficiency})^{CT}$. The slope of the standard curve and cycle thresholds (CTs) were analyzed using ABI PRISM 7500 SDS software. Expression of Dnmt3a was normalized to β-actin as an internal control. At least three independent PCRs were performed in duplicate for all samples.

Protein Extraction and Western Blotting

Mouse EBs and ESCs were lysed in RIPA buffer (50 mM Tris-HCl [pH 8.0], 400 mM NaCl, 1% Nonident P-40, 1% sodium deoxycholate, 0.1% SDS, 1 mM phenylmethylsulfonyl fluoride, 5 μg/ml leupeptin, 1 μg/ml aprotinin, 5 μg/ml pepstatin, 0.5 mM EDTA, and 0.5 mM NaF). The lysates were clarified by centrifugation at 15,000 rpm for 30 minutes at 4°C, and 5-μg aliquots of the lysates were subjected to SDS polyacrylamide gel electrophoresis on 7.5%

gel. Protein concentration was determined by using a bicinchoninic acid protein assay kit (Pierce Chemical, Rockford, IL, http://www.piercenet.com) according to the manufacturer's instructions. The proteins were transferred to polyvinylidene difluoride membrane and probed with 1:125 diluted anti-Dnmt3a monoclonal antibody (clone 64B1446; Imgenex, San Diego, http://www.Imgenex.com) or 1:1,000 diluted anti-glyceraldehyde-3-phosphate dehydrogenase monoclonal antibody (Imgenex) as the first antibody and 1:5,000 diluted anti-mouse immunoglobulins conjugated with horseradish peroxidase (Wako Pure Chemicals) as the second antibody. The anti-Dnmt3a monoclonal antibody recognizes two Dnmt3a subtypes, Dnmt3a and Dnmt3a2 [36]. The chemiluminescence signals, which were obtained with SuperSignal West Pico Chemiluminescent Substrate (Pierce Chemical), were visualized by Chemi-Smart 3000 (Vilber Lourmat, Marne-la-Vallée, France, http://www.vilber.com). For reprobing, the blotted membrane was rinsed with Restore Western Blot Stripping Buffer (Pierce Chemical).

Preparation of Genomic DNA

Genomic DNA was extracted as previously described [37]. Briefly, cells were suspended in lysis buffer (150 mM EDTA, 10 mM Tris-HCl [pH 8.0], and 1% SDS) containing 10 mg/ml proteinase K (Merck, Darmstadt, Germany, http://www.merck.com). The mixture was incubated at 55°C for 20 minutes. After two phenol/chloroform/isoamyl alcohol (50:49:1) extractions, genomic DNA was precipitated in ethanol and dissolved in TE buffer (10 mM Tris-HCl, 1 mM EDTA [pH 8.0]).

Restriction Landmark Genomic Scanning

The restriction landmark genomic scanning (RLGS) was performed using the restriction enzyme combination of Not I, Pvu II, and Pst I as described previously [38]. Genomic DNA was treated with Klenow fragment (Takara, Kyoto, Japan, http://www.takara-bio.com) in the presence of dGTPαS, dCTPαS (GE Healthcare, Little Chalfont, Buckinghamshire, UK, http://www.gehealthcare.com), ddATP, and ddTTP (Takara) to prevent nonspecific labeling. After digestion by Not I as a landmark enzyme (Nippon Gene, Toyama, Japan, http://www.nippongene.com), cohesive ends were isotopically labeled with Sequenase Ver 2.0 (USB Corporation, Cleveland, http://www.usbweb.com) in the presence of [α-^{32}P]dCTP and [α-^{32}P]dGTP (GE Healthcare). Labeled DNA was digested by Pvu II (Nippon Gene) after first dimensional electrophoresis in 0.9% agarose disc gel. After in-gel digestion with Pst I (Nippon Gene), the DNA fragments were separated by a second dimensional electrophoresis in a polyacrylamide slab gel. The gel was then dried and exposed to x-ray film (Kodak, XAR 5; Eastman Kodak, Rochester, NY, http://www.kodak.com) for 2–3 weeks at −80°C.

Methylation-Sensitive Quantitative Real-Time PCR

DNA methylation status at *Sall3* locus was evaluated using methylation-sensitive quantitative real-time PCR as previously described [39]. Twenty nanograms of DNA treated with or without Not I was subjected to PCR with a primer pair amplifying a genomic fragment containing the Not I site. The methylation ratio was determined as the proportion of undigested DNA in Not I-treated DNA to that in Not I-untreated DNA. The amplification was monitored with SYBR green on an ABI Prism 7500 Sequence Detection System (Applied Biosystems) following the manufacturer's protocol. Initial DNA amount in the reaction mix was normalized with the value obtained with the primer pair of Xist1 that was designed to amplify fragments without the Not I site. More than three independent PCRs in triplicate were performed. The primers of Sall3 and Xist1 are as follows: Sall3: 5′-TTATACAACCTCGAACTAGCTGGG-3′ and 5′-GCATCCTGAATCCATGAACCCT-3′, Xist1: 5′-CACACACACCCTGCCCAATC-3′ and 5′-GGGATTCGCCTTGATTTGTGGT-3′.

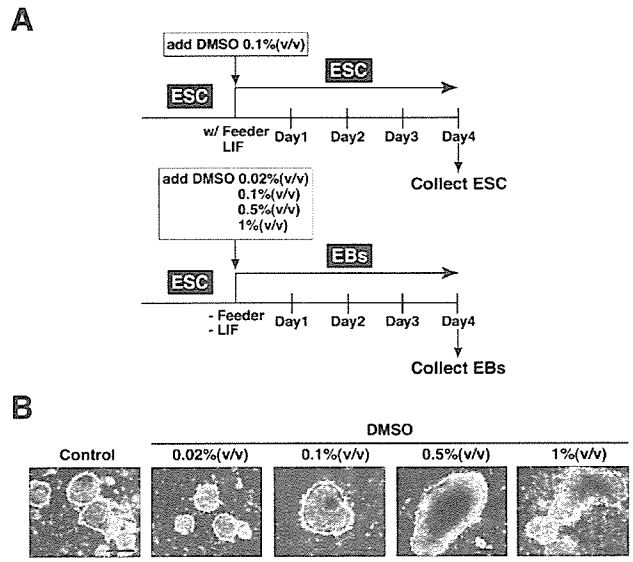

Figure 1. Culture of ESCs and of EBs with or without DMSO. **(A):** Cultivation scheme of mouse ESCs (MS12 line) and EBs. ESCs were cultured for 4 days in the presence of LIF and feeder layer with or without DMSO, or were induced to form EBs by removal of LIF and feeder layer, and were cultured for another 4 days with various concentrations of DMSO. **(B):** Micrographs of EBs cultured in medium containing DMSO. Concentrations are indicated above the images. Scale bars = 200 μm. Abbreviations: DMSO, dimethyl sulfoxide; EB, embryoid body; ESC, embryonic stem cell; LIF, leukemia inhibitory factor.

Southern Blot Hybridization

Genomic DNA that was digested with Msp I (Takara) or Hap II (Takara) was electrophoresed on a 0.8% agarose gel. After being hydrolyzed with 0.25 N HCl and denatured with 1.5 M NaCl in 0.5 N NaOH, DNA was transferred to a nylon membrane. The membrane was hybridized with pMO for endogenous C-type retrovirus (MoMuLV) (GenBank accession: NC_001501) or pMR150 for minor satellite repeats (X14469 and X07949), which was labeled with Gene Images random prime labeling module (GE Healthcare). The bound probes were detected by using Gene Images CDP-star detection module (GE Healthcare) with x-ray film (RX-U; Fuji, Kanagawa, Japan, http://www.fujifilm.com).

Results

DMSO Increases Expression of Dnmt3as in ESCs and EBs

ESCs, which were maintained without DMSO treatment, were cultured under differentiation conditions to form 4-day EBs in the absence or presence of various concentrations (0.02%–1%) of DMSO (Fig. 1A). In contrast to uniform spheres of EBs

cultured without DMSO, EBs with irregular shapes and increased sizes appeared in high concentrations (0.5%, 1%) of DMSO (Fig. 1B). In these phenotype changes of EBs induced by DMSO, we presume that epigenetic systems should be involved.

By semiquantitative RT-PCR, we examined expression of genes related to epigenetic systems such as Dnmts and histone modification enzymes. mRNA levels of Dnmt1 and Dnmt3b, which were expressed in ESCs and EBs, were not affected by DMSO treatment as judged by the densitometry of RT-PCR products (Fig. 2A). The fold changes of intensities of bands between the control and 1% DMSO-treated EBs showed 1.10 and 0.93 for Dnmt1 and Dnmt3b, respectively. In spite of the report that mDot1 mRNA was increased by DMSO treatment in mIMCD cells [25], mRNAs for histone methyltransferases (G9a, Suv39h1, Suv39h2, and mDot1), and a histone deacetylase, Sir2α, were expressed equally in ESCs as well as EBs at different DMSO concentrations. On the contrary, intensities of Dnmt3a in EBs, treated with 0.5% and 1% DMSO, increased almost double.

Real-time quantitative RT-PCR confirmed the increase of Dnmt3a mRNA (Fig. 2B). In ESCs, 0.1% of DMSO treatment caused a slight increase in the level of Dnmt3a mRNA. An approximately twofold increase in Dnmt3a mRNA was observed by differentiation of ESCs to EBs. In EBs, statistically significant increases in levels of Dnmt3a mRNA corresponded to increases in DMSO dosage.

To address the question whether Dnmt3a protein would increase coordinately with transcripts of Dnmt3a by DMSO treatment, Dnmt3a proteins in EBs were analyzed by Western blotting. Two distinct bands, which were detected by anti-Dnmt3a monoclonal antibody, indicated the expression of Dnmt3a and Dnmt3a2 in 4-day EBs. Both types of Dnmt3a protein levels in EBs treated with 0.5% and 1% DMSO increased to two times those in nontreated EBs (Fig. 2C). From this finding, taken together with upregulated mRNA level by DMSO treatment, it was clear that DMSO increased expression of Dnmt3as (Dnmt3a and Dnmt3a2).

DMSO Affects DNA Methylation Status of Repetitive Sequences in EBs

The mammalian genome consists of genic and nongenic regions, such as repetitive sequences, and the latter occupy a large part of the genome. Both regions are methylated de novo by Dnmt3as [40]. Minor satellite repeats, which are located in the centromeric regions, and endogenous retroviruses, which are interspersed in the mouse genome, are families of repetitive sequences. To assess the effects of DMSO (0.1%) on methylation levels in EBs, Southern blot was performed using probes for minor satellite repeats (pMR150) and endogenous C-type retroviruses (pMO) (Fig. 3). The differences in amounts of small fragments between lanes I, DNA digested by a DNA methylation-insensitive restriction enzyme, Msp I, and lanes II, digested by a methylation-sensitive enzyme, Hap II, indicate that these repetitive sequences were hypermethylated in EBs. The 0.1% DMSO treatment caused the disappearance of the small fragments of minor satellite and C-type retrovirus repeats in the EB genome (lanes III). These data indicated that DMSO prompted DNA methylation of these nongenic regions in the EBs.

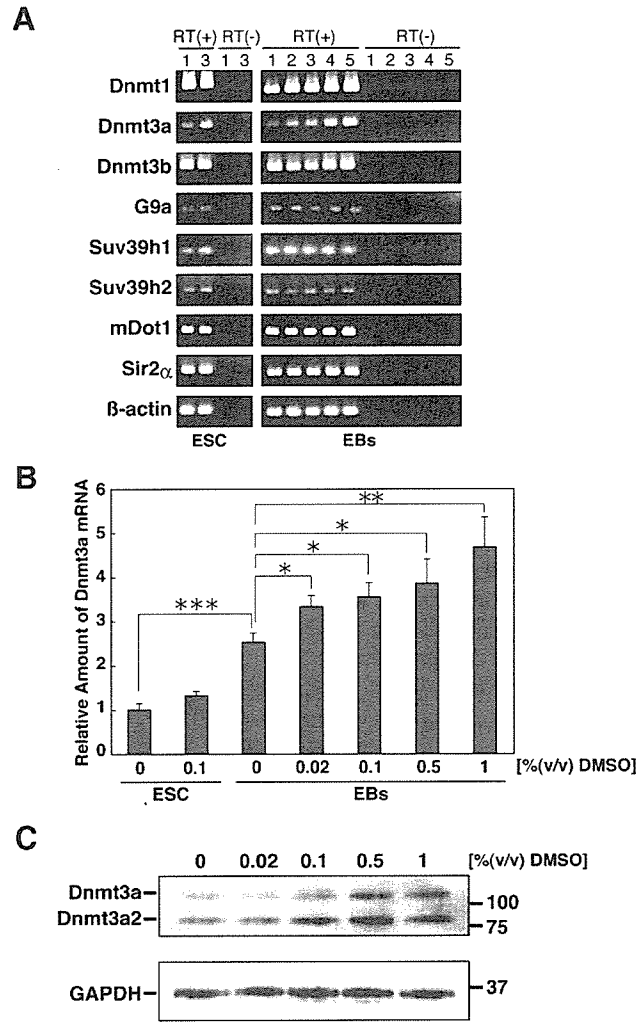

Figure 2. The effects of DMSO on expression of epigenetic factors in ESCs and EBs. **(A):** Expression of epigenetic factors in ESCs and EBs was analyzed by reverse transcription-polymerase chain reaction (RT-PCR). Reactions were carried out with [RT(+)] or without [RT(-)] reverse transcriptase. Primer sets are indicated to the left of the gel images. Concentrations (vol/vol) of DMSO were 0% (lane 1), 0.02% (lane 2), 0.1% (lane 3), 0.5% (lane 4), and 1% (lane 5). **(B):** Dnmt3a expression was analyzed by real-time quantitative RT-PCR. The value obtained in ESCs without DMSO was set to 1. Shaded blocks represent mean values, and standard error is represented by vertical bars. Differences between samples were analyzed by t test (*$p < .1$, **$p < .05$, ***$p < .005$ [$n = 3$]). **(C):** Dnmt3a protein expression was analyzed by Western blotting. The positions of proteins (left side) and molecular weights of the markers (right side) are shown. Abbreviations: DMSO, dimethyl sulfoxide; Dnmt, DNA methyltransferase; EB, embryoid body; ESC, embryonic stem cell; GAPDH, glyceraldehyde-3-phosphate dehydrogenase.

DMSO Affects Genome-Wide DNA Methylation Profiles of Genic Areas in EBs

Next, we focused on the effect of DMSO on DNA methylation at the genic region using the RLGS method. In the RLGS profile, the spot is visible when the corresponding cutting site of Not I, a methylation-sensitive restriction enzyme, is hypomethylated, whereas it is invisible when the site is hypermethylated. Most Not I sites are in CpG islands [41], which are characterized by high CG content and frequent CpG appearance [42], and are

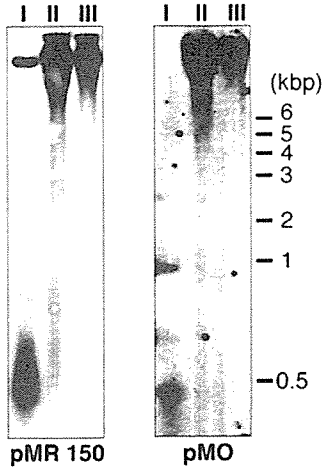

Figure 3. Effect of dimethyl sulfoxide (DMSO) on DNA methylation status of repetitive sequences. Msp I-digested genomic DNA from untreated EBs (lane I) and Hap II-digested genomic DNA from untreated (lane II) and 0.1% (vol/vol) DMSO-treated EBs (lane III) were subjected to Southern blot hybridization using probes for minor satellite repeats (pMR150) and endogenous C-type retrovirus repeats (pMO). Molecular weights are indicated on the right panel.

often localized at promoter regions of housekeeping genes and many tissue-specific genes [42–44]. Therefore, RLGS enables us to simultaneously analyze thousands of loci in genic regions.

The RLGS profiles, consisting of approximately 1,500 spots, were compared between control and 0.1% DMSO-treated EBs (Fig. 4A). In RLGS profiles of DMSO-treated EBs, 11 unique spots (T-DMR [DMSO] 1–11) emerged, indicating that DMSO induced hypomethylation of these 11 sites in EBs (Fig. 4B). In contrast, four spots (T-DMRs [DMSO] 12–15) disappeared in DMSO-treated EBs, indicating that DMSO caused hypermethylation of these four sites. Thus, 15 genomic loci were epigenetically affected by DMSO treatment, whereas thousands of loci remained unchanged (Fig. 4A, 4B).

We compared these 15 spots (T-DMRs [DMSO] 1–15) with T-DMRs that we previously identified [15, 16] (Fig. 5). The two spots, T-DMRs (DMSO) 2 and 12, were matched with T-DMRs 148 and 253, respectively, whereas the other 13 spots were novel. We defined them as T-DMRs 582 and 701–712, serially (Fig. 5). One of the matched spots is located in *Sall3* gene (T-DMR [DMSO] 2), which is specifically hypermethylated in the trophoblast lineage but hypomethylated in ESCs [31]. By methylation-sensitive PCR, DNA methylation status of this locus in DMSO-treated EBs was estimated to be approximately 3.5 times lower than that in EBs without DMSO (Fig. 4C).

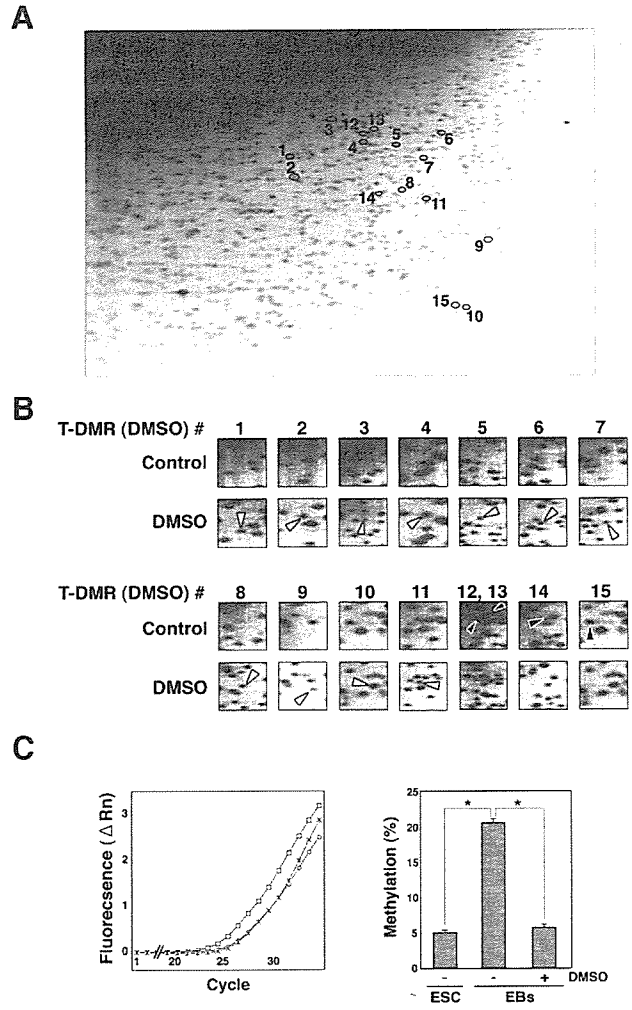

Figure 4. Analysis of genome-wide DNA methylation status in mouse EBs untreated or treated with DMSO and methylation status of *Sall3* locus. **(A):** RLGS profile obtained with genomic DNA of EBs treated with 0.1% (vol/vol) of DMSO. The 15 spots, which differentially appeared by treatment with DMSO, are marked with numbered circles. **(B):** Higher magnification of the RLGS profile. The 11 RLGS spots that emerged (i.e., hypomethylated) and the four spots that disappeared (i.e., hypermethylated) by DMSO treatment are indicated with white and black arrowheads, respectively. **(C):** Methylation-sensitive quantitative real-time PCR analysis for *Sall3* locus. Amplification curves with asterisks, circles, and squares represent Not I-treated genomic DNA of ESCs and of EBs with or without DMSO treatment, respectively (left panel). Methylation levels of *Sall3* locus were estimated as described in Materials and Methods. Differences between samples were statistically analyzed by *t* test (*$p < .001$, [ESCs: $n = 3$, EBs: $n = 4$]) (right panel). Abbreviations: DMSO, dimethyl sulfoxide; ΔRn, delta normalized reporter; EB, embryoid body; ESC, embryonic stem cell; PCR, polymerase chain reaction; RLGS, restriction landmark genomic scanning; T-DMR, tissue-dependent and differentially methylated region.

Discussion

The present study clearly demonstrates that DMSO has an impact on the epigenetic regulatory system, changes the genome-wide DNA methylation status, and induces formation of structurally abnormal EBs. Irreversible phenotypic changes in Friend cells were induced by DMSO [2, 3]. In animal cloning technology, DMSO improved the frequency of development to blastocyst stage and full term [5]. Because DNA methylation plays a critical role in mouse development and the definition of cell properties, change in genome-wide DNA methylation profiles induced by DMSO treatment may be responsible for these phenomena.

The human and mouse genomes contain 30,000–40,000 genes; however, genes occupy only a small percentage of the approximately 3×10^9 bp haploid genome. In contrast, 41%–48% of the mammalian genome is composed of nongenic repetitive elements, including satellites interspersed repeats such

T-DMR (DMSO) number	1	2	3	4	5	6	7	8	9	10	11	12	13	14	15
T-DMR number	582	148	701	702	703	704	705	706	707	708	709	253	710	711	712
ESC	○	○	○	○	○	○	○	○	○	○	○	●	●	●	○
EB 4day (control)	●	●	●	●	●	●	●	●	●	●	●	○	○	○	○
EB 4day (DMSO)	○	○	○	○	○	○	○	○	○	○	○	●	●	●	●

○: spot appeared on RLGS profile (unmethylated status).
●: no spot on RLGS profile (methylated status).

Figure 5. Matching of T-DMRs (DMSO) to previously identified T-DMRs. T-DMRs (DMSO) 1–15 (Fig. 4) were compared with previously identified T-DMRs by matching RLGS profiles. T-DMRs (DMSO) 2 and 12 correspond to T-DMRs 148 and 253 (which were previously identified), respectively. The 13 novel RLGS spots—T-DMRs (DMSO) 1, 3–11, and 13–15—were designated as T-DMRs 582 and 701–712, serially. Abbreviations: DMSO, dimethyl sulfoxide; EB, embryoid body; ESC, embryonic stem cell; RLGS, restriction landmark genomic scanning; T-DMR, tissue-dependent and differentially methylated region.

as retroviruses [45, 46]. A recent database analysis suggested that approximately half of all promoter regions are located in CpG islands [44]. We have identified many regions in CpG islands that have different methylation statuses depending on cell types and tissues, indicating that dynamic change in DNA methylation occurs during differentiation [15–17]. The present study demonstrated that DMSO impacts DNA methylation status genome-wide, including genic and nongenic regions of EBs differentiated from ESCs. Furthermore, hypermethylation as well as hypomethylation occurred at 15 independent genomic loci after DMSO treatment. However, note that there are approximately 15,500 CpG islands in the mouse genome [46], which suggests that the methylation status of many loci must be affected by DMSO.

Differentiation of ESCs to EBs causes both hypermethylation and hypomethylation at various loci genome-wide in mammals [16]. The effects of DMSO on DNA methylation status of CpG islands during differentiation are summarized in Figure 6. When ESCs differentiate to EBs, 34 loci were hypermethylated, and 30 loci were hypomethylated, whereas 203 spots were unchanged. Of 34 loci that typically became hypermethylated during differentiation of ESCs to EBs, 11 remained hypomethylated after DMSO treatment. Similarly, the DNA methylation status of three out of the 30 hypomethylated loci, and one out of the 203 unchanged loci was affected by DMSO treatment. Thus, DMSO induces alteration of DNA methylation status at selected loci and generates a unique DNA methylation profile of EBs, accompanying the abnormal phenotypes.

We demonstrated the upregulation of mRNA and protein expression in Dnmt3as by DMSO. Overexpression of Dnmt3as causes de novo hypermethylation of both genic and nongenic regions in vivo [40]. Abnormal expression of Dnmts has been observed in cancerous cells in which aberrant DNA methylation occurred; such expression includes an increase in DNMT1 and DNMT3b expression in various cancer cells [47] and a higher level of DNMT3a expression in leukemia [48, 49]. The preference of Dnmts for target loci within CpG islands was observed in ESCs [39]. Catalytic activities of Dnmt3a showed preference for nucleotide composition around the CpG sites [50]. Therefore, DMSO-induced increased expression of Dnmt3as should be involved in hypermethylation occurring at nongenic regions and selected gene loci of EB genome.

Despite increased expression of Dnmt3as and hypermethylation of the repetitive sequences and the selected loci, a number of hypomethylated loci (11 spots) are greater than that of hypermethylated loci (four spots) in genic regions (Fig. 4). In many cancer cells with epigenetic abnormalities, genomic DNA has shown to be globally hypomethylated with

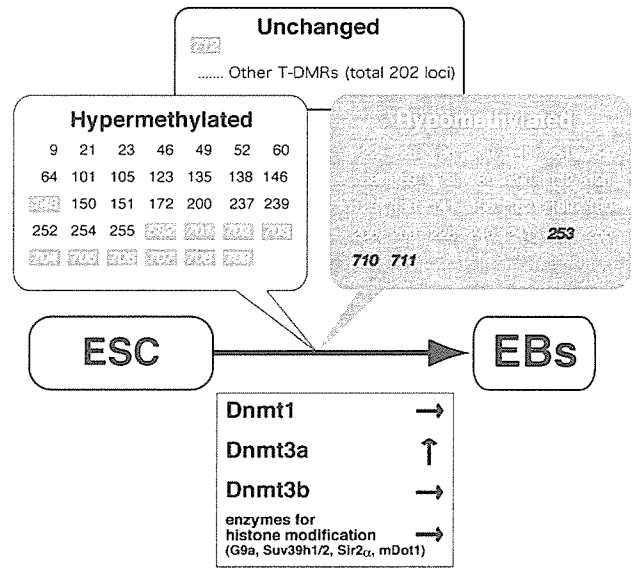

Figure 6. The impact of dimethyl sulfoxide (DMSO) on tissue-dependent and differentially methylated region (T-DMRs). This figure illustrates the T-DMRs that were hypermethylated, hypomethylated, or unchanged during the differentiation of ESCs into EBs. T-DMRs with methylation status affected by DMSO are in bold italics. Numbers with white letters in shaded square boxes and numbers with black letters in the shaded balloon represent hypomethylated and hypermethylated loci by DMSO, respectively. Abbreviations: Dnmt, DNA methyltransferase; EB, embryoid body; ESC, embryonic stem cell.

hypermethylation at selected genes. Such locus-specific DNA methylation status on genomic loci is contributed by complex combinations of Dnmts and other epigenetic regulators. Dnmt1 and Dnmt3s functionally cooperate with each other during methylation of genomic DNA [51, 52]. Methylation of DNA, however, was not solely regulated by Dnmts; chromatin configuration affects DNA methylation status and vice versa [20, 22–24]. Therefore, genome-wide alteration of the DNA methylation profile by DMSO should not be explained simply by the increased levels of Dnmt3as.

Conclusion

We conclude that DMSO upregulates expression of Dnmt3as and affects DNA methylation status at restricted loci accompanied with abnormal EB formation. Physiological and toxicological assessment of chemical agents at epigenetic levels is important, and analysis of genome-wide DNA methylation profiles will be useful in evaluating epimutagens.

ACKNOWLEDGMENTS

We thank Dr. Maddy Roberts and Chiaki Maeda for proofreading the original manuscript. This work was supported by the Program for Promotion of Basic Research Activities for Innovative Biosciences, Health Science Research Grant from the Ministry of Health, Labor and Welfare of Japan, and the Grant-in-aid for Scientific Research, Ministry of Education, Culture, Sports, Science and Technology, Japan (15208027, 15080202) (to K.S.).

DISCLOSURES

The authors indicate no potential conflicts of interest.

REFERENCES

1 Santos NC, Figueira-Coelho J, Martins-Silva J et al. Multidisciplinary utilization of dimethyl sulfoxide: Pharmacological, cellular, and molecular aspects. Biochem Pharmacol 2003;65:1035–1041.

2 Preisler HD, Giladi M. Differentiation of erythroleukemic cells in vitro: Irreversible induction by dimethyl sulfoxide (DMSO). J Cell Physiol 1975;85:537–546.

3 Gusella J, Geller R, Clarke B et al. Commitment to erythroid differentiation by friend erythroleukemia cells: A stochastic analysis. Cell 1976; 9:221–229.

4 Edwards MK, Harris JF, McBurney MW. Induced muscle differentiation in an embryonal carcinoma cell line. Mol Cell Biol 1983;3:2280–2286.

5 Wakayama T, Yanagimachi R. Effect of cytokinesis inhibitors, DMSO and the timing of oocyte activation on mouse cloning using cumulus cell nuclei. Reproduction 2001;122:49–60.

6 Hattori N, Nishino K, Ko YG et al. Epigenetic control of mouse Oct-4 gene expression in embryonic stem cells and trophoblast stem cells. J Biol Chem 2004;279:17063–17069.

7 Nishino K, Hattori N, Tanaka S et al. DNA methylation-mediated control of Sry gene expression in mouse gonadal development. J Biol Chem 2004;279:22306–22313.

8 Sinsheimer RL. The action of pancreatic deoxyribonuclease. II. Isomeric dinucleotides J Biol Chem 1955;215:579–583.

9 Russo VEA, Martienssen RA, Riggs AD. Introduction. In: Russo VEA, Martienssen RA, Riggs AD, eds. Epigenetic Mechanisms of Gene Regulation. Woodbury, NY: Cold Spring Harbor Laboratory Press, 1996: 1–4.

10 Bird AP, Wolffe AP. Methylation-induced repression–belts, braces, and chromatin. Cell 1999;99:451–454.

11 Bird A. DNA methylation patterns and epigenetic memory. Genes Dev 2002;16:6–21.

12 Lachner M, Jenuwein T. The many faces of histone lysine methylation. Curr Opin Cell Biol 2002;14:286–298.

13 Imamura T, Ohgane J, Ito S et al. CpG island of rat sphingosine kinase-1 gene: Tissue-dependent DNA methylation status and multiple alternative first exons. Genomics 2001;76:117–125.

14 Futscher BW, Oshiro MM, Wozniak RJ et al. Role for DNA methylation in the control of cell type specific maspin expression. Nat Genet 2002; 31:175–179.

15 Shiota K, Kogo Y, Ohgane J et al. Epigenetic marks by DNA methylation specific to stem, germ and somatic cells in mice. Genes Cells 2002;7:961–969.

16 Kremenskoy M, Kremenska Y, Ohgane J et al. Genome-wide analysis of DNA methylation status of CpG islands in embryoid bodies, teratomas, and fetuses. Biochem Biophys Res Commun 2003;311:884–890.

17 Shiota K. DNA methylation profiles of CpG islands for cellular differentiation and development in mammals. Cytogenet Genome Res 2004; 105:325–334.

18 Okano M, Xie S, Li E. Dnmt2 is not required for de novo and maintenance methylation of viral DNA in embryonic stem cells. Nucleic Acids Res 1998;26:2536–2540.

19 Hata K, Okano M, Lei H et al. Dnmt3L cooperates with the Dnmt3 family of de novo DNA methyltransferases to establish maternal imprints in mice. Development 2002;129:1983–1993.

20 Li E. Chromatin modification and epigenetic reprogramming in mammalian development. Nat Rev Genet 2002;3:662–673.

21 Chen T, Li E. Structure and function of eukaryotic DNA methyltransferases. Curr Top Dev Biol 2004;60:55–89.

22 Xin Z, Tachibana M, Guggiari M et al. Role of histone methyltransferase G9a in CpG methylation of the Prader-Willi syndrome imprinting center. J Biol Chem 2003;278:14996–15000.

23 Lehnertz B, Ueda Y, Derijck AA et al. Suv39h-mediated histone H3 lysine 9 methylation directs DNA methylation to major satellite repeats at pericentric heterochromatin. Curr Biol 2003;13:1192–1200.

24 Espada J, Ballestar E, Fraga MF et al. Human DNA methyltransferase 1 is required for maintenance of the histone H3 modification pattern. J Biol Chem 2004;279:37175–37184.

25 Zhang W, Hayashizaki Y, Kone BC. Structure and regulation of the mDot1 gene, a mouse histone H3 methyltransferase. Biochem J 2004; 377:641–651.

26 Vaquero A, Scher M, Lee D et al. Human SirT1 interacts with histone H1 and promotes formation of facultative heterochromatin. Mol Cell 2004; 16:93–105.

27 Hansen RS, Wijmenga C, Luo P et al. The DNMT3B DNA methyltransferase gene is mutated in the ICF immunodeficiency syndrome. Proc Natl Acad Sci U S A 1999;96:14412–14417.

28 Shahbazian MD, Zoghbi HY. Rett syndrome and MeCP2: Linking epigenetics and neuronal function. Am J Hum Genet 2002;71:1259–1272.

29 Ohgane J, Wakayama T, Kogo Y et al. DNA methylation variation in cloned mice. Genesis 2001;30:45–50.

30 Humpherys D, Eggan K, Akutsu H et al. Epigenetic instability in ES cells and cloned mice. Science 2001;293:95–97.

31 Ohgane J, Wakayama T, Senda S et al. The Sall3 locus is an epigenetic hotspot of aberrant DNA methylation associated with placentomegaly of cloned mice. Genes Cells 2004;9:253–260.

32 Jones PA, Baylin SB. The fundamental role of epigenetic events in cancer. Nat Rev Genet 2002;3:415–428.

33 Holliday R. Mutations and epimutations in mammalian cells. Mutat Res 1991;250:351–363.

34 O'Shea KS. Embryonic stem cell models of development. Anat Rec 1999;257:32–41.

35 Kawase E, Suemori H, Takahashi N et al. Strain difference in establishment of mouse embryonic stem (ES) cell lines. Int J Dev Biol 1994;38: 385–390.

36 Chen T, Ueda Y, Xie S et al. A novel Dnmt3a isoform produced from an alternative promoter localizes to euchromatin and its expression correlates with active de novo methylation. J Biol Chem 2002;277: 38746–38754.

37 Ohgane J, Aikawa J, Ogura A et al. Analysis of CpG islands of trophoblast giant cells by restriction landmark genomic scanning. Dev Genet 1998;22:132–140.

38 Ohgane J, Hattori N, Shiota K. Analysis of tissue-specific DNA methylation during development. Methods Mol Biol 2005;289:371–382.

39 Hattori N, Abe T, Hattori N et al. Preference of DNA methyltransferases for CpG islands in mouse embryonic stem cells. Genome Res 2004;14: 1733–1740.

40 Chen T, Ueda Y, Dodge JE et al. Establishment and maintenance of genomic methylation patterns in mouse embryonic stem cells by Dnmt3a and Dnmt3b. Mol Cell Biol 2003;23:5594–5605.

41 Fazzari MJ, Greally JM. Epigenomics: Beyond CpG islands. Nat Rev Genet 2004;5:446–455.

42 Gardiner-Garden M, Frommer M. CpG islands in vertebrate genomes. J Mol Biol 1987;196:261–282.

43 Larsen F, Gundersen G, Lopez R et al. CpG islands as gene markers in the human genome. Genomics 1992;13:1095–1107.

44 Suzuki Y, Tsunoda T, Sese J et al. Identification and characterization of the potential promoter regions of 1031 kinds of human genes. Genome Res 2001;11:677–684.

45 Lander ES, Linton LM, Birren B et al. Initial sequencing and analysis of the human genome. Nature 2001;409:860–921.

46 Waterston RH, Lindblad-Toh K, Birney E et al. Initial sequencing and comparative analysis of the mouse genome. Nature 2002;420:520–562.

47 Kanai Y, Ushijima S, Kondo Y et al. DNA methyltransferase expression and DNA methylation of CPG islands and peri-centromeric satellite regions in human colorectal and stomach cancers. Int J Cancer 2001;91: 205–212.

48 Mizuno S, Chijiwa T, Okamura T et al. Expression of DNA methy ltransferases DNMT1, 3A, and 3B in normal hematopoiesis and in acute and chronic myelogenous leukemia. Blood 2001;97:1172–1179.

49 Tessema M, Langer F, Dingemann J et al. Aberrant methylation and impaired expression of the p15(INK4b) cell cycle regulatory gene in chronic myelomonocytic leukemia (CMML). Leukemia 2003;17:910–918.

50 Lin IG, Han L, Taghva A et al. Murine de novo methyltransferase Dnmt3a demonstrates strand asymmetry and site preference in the methylation of DNA in vitro. Mol Cell Biol 2002;22:704–723.

51 Liang G, Chan MF, Tomigahara Y et al. Cooperativity between DNA methyltransferases in the maintenance methylation of repetitive elements. Mol Cell Biol 2002;22:480–491.

52 Kim GD, Ni J, Kelesoglu N et al. Co-operation and communication between the human maintenance and de novo DNA (cytosine-5) methyltransferases. Embo J 2002;21:4183–4195.